Non-parabolic intergranular barriers in tin oxide and gas sensing

C. M. Aldao and C. Malagù

Citation: J. Appl. Phys. **112**, 024518 (2012); doi: 10.1063/1.4739490
View online: http://dx.doi.org/10.1063/1.4739490
View Table of Contents: http://jap.aip.org/resource/1/JAPIAU/v112/i2
Published by the American Institute of Physics.

Non-parabolic intergranular barriers in tin oxide and gas sensing

C. M. Aldao[1,a)] and C. Malagù[2]
[1]*Institute of Materials Science and Technology (INTEMA), University of Mar del Plata and National Research Council (CONICET), Juan B. Justo 4302, B7608FDQ Mar del Plata, Argentina*
[2]*Department of Physics, University of Ferrara, Via Saragat, 1-44100 Ferrara, Italy*

(Received 3 April 2012; accepted 27 June 2012; published online 30 July 2012)

Chemoresistive properties of crystalline solids strongly depend on the concentration of stoichiometric defects. In the case of tin oxide, oxygen vacancies are a case in point of such kind of defects. We address the problem of band bending and Schottky barrier formation in tin oxide. We approached the problem of charged native defects, oxygen vacancies, in a metal oxide in equilibrium with an oxygen containing ambient under three equivalent points of view. We focused on the non-parabolic barriers character that forms at intergrains. Implications in electrical responses to oxygen concentration variations will be discussed. © *2012 American Institute of Physics*. [http://dx.doi.org/10.1063/1.4739490]

INTRODUCTION

Tin oxide is used in the detection of diverse gases that can be detected through changes in the film conductivity. It is well known that oxygen can be chemisorbed at grains surfaces as charged species affecting intergranular potential barriers that control the film conductivity and then its sensor abilities.[1–5] Thus, the sensing mechanism is mainly based on the surface reactions that involve chemisorbed species.[6–8] It is generally accepted that barriers formed between grains are responsible for the sensor conductivity and that they have a Schottky-type nature.[2] Researchers have regularly considered a conductivity of the type

$$G = G_0 \exp(-eV_s/kT) \tag{1}$$

that reflects an activated process due to intergranular barriers and holds for many metal oxide semiconductors.

Since intergrains are responsible for the film conductivity, the understanding and control of the surface and near-surface electronic phenomena are the key to improve the sensitivity of sensor devices. We will focus here on the basic phenomena taking place at the grains related to the dependence of the surface barriers in tin oxide on the oxygen pressure of the gas phase.

It is generally accepted that oxygen adsorption at the grains surfaces directly reflects on band bending by assuming parabolic barriers due to a constant density of donors along the depletion region. However, the equilibrium oxygen vacancies density is far from constant implying a particular dependence on the amount of adsorbed oxygen and then on the ambient oxygen pressure. On the other hand, in previous works[10–14] we have demonstrated that not only thermionic emission is responsible for conductance but also tunneling has to be taken into account to explain observed changes in resistance. This is why we are very interested not only on the barriers height but also on the shape of the barriers, as tunneling depends on both.

Using three approaches, we will find out the native defects (oxygen vacancies) density in a metal oxide in equilibrium with an oxygen containing ambient. We will show that it is far from constant along the depletion region and, consequently, surface barriers are not parabolic. Based on these results, we will determine intergranular barriers as a function of oxygen pressure to compare with recent experiments. Finally, we will calculate the surface barrier modifications due to oxygen diffusion into the grain, which are consistent with a slow change in the sample resistivity as experimentally observed.

OXYGEN VACANCY CONCENTRATION

It is well established that tin oxide is a wide band-gap (3.6 eV) semiconductor of *n*-type due to oxygen deficiency. Indeed, oxygen vacancies are the dominant defects and they behave as donor impurities. Figure 1 shows an n-type semiconductor with surface states that can acquire a negative charge. The curvature of the bands is the band bending due to the positive charge at the depletion region (between $x = 0$ and x_0) and the negatively charged surface states. We will show that band bending has a tremendous effect on the equilibrium oxygen vacancy concentration.

The oxygen exchange equilibrium between SnO_2 with the gas phase is regularly written as[9]

$$O_0 \Longleftrightarrow V^{++} + 2e^- + \frac{1}{2}O_2, \tag{2}$$

where O_0 is the neutral oxygen at the crystal, V^{++} is a doubly ionized oxygen vacancy, e^- is an electron, and O_2 an oxygen molecule at the gas phase. Equation (2) implies several mechanisms, as the density of vacancies must be able to evolve to reach equilibrium (for example, after a change of the oxygen pressure or temperature). These mechanisms can be the following. First, neutral oxygen in the crystal leaves its position to create a doubly ionized vacancy and a doubly ionized interstitial

a)Author to whom correspondence should be addressed. Electronic mail: cmaldao@fi.mdp.edu.ar.

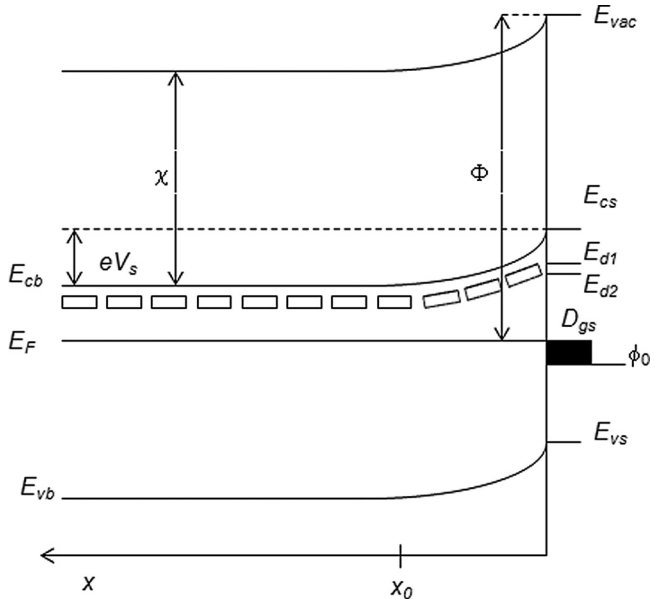

FIG. 1. Bands at a semiconductor surface illustrating the formation of the space charge region. ϕ is the work function, χ is the electron affinity, eV_s is the band bending, D_{gs} represents surface states, E_{d1} and E_{d2} are the donor levels, and ϕ_0 is the neutral level for surface states.

$$O_0 \Longleftrightarrow V^{++} + O_i^{--}. \tag{3}$$

Then, oxygen interstitials migrate to the surface

$$O_i^{--} + S \Longleftrightarrow O_s^{--}, \tag{4}$$

where$S$ denotes a surface site. (We could also consider that the main adsorbed charged oxygen species is O^-.)

Ionized oxygen at the surface becomes neutral

$$O_s^{--} \Longleftrightarrow O_s^0 + 2e^-. \tag{5}$$

Finally, adsorbed oxygen desorbs to the gas phase

$$O_s^0 \Longleftrightarrow \frac{1}{2}O_2 + S. \tag{6}$$

Under thermodynamic equilibrium, the corresponding mass action law for Eq. (2) is written as

$$K = [V^{++}]n^2\, p(O_2)^{1/2}. \tag{7}$$

Square brackets denote concentration, n is the electron density, and $p(O_2)$ is the oxygen partial pressure. K is the mass action constant that is related to the energy involved in the reaction

$$K \propto \exp[(-E_{for} + E_{d1} + E_{d2} - 2E_c)/kT], \tag{8}$$

where E_{for} is the energy needed to take an atom from a lattice site inside the crystal to the vapor phase, E_{d1} and E_{d2} are the donor levels, and E_c is the bottom of the conduction band.

Equation (7) implies that the product $[V^{++}]n^2$ remains constant for a given value of oxygen pressure. This relation has tremendous implications on the intergranular barriers because the vacancy concentration near the surface can be very different from that at the bulk due to band bending. K does not depend on the relative position of the Fermi level with respect to the bands, but $[V^{++}]$ does because of n. Since n is proportional to $\exp[-(E_c - E_F)/\mathrm{kT}]$, from Eq. (7) the vacancy density can be written as

$$[V^{++}] \propto p(O_2)^{-1/2}\exp[(-E_{for} + E_{d1} + E_{d2} - 2E_F)/kT]. \tag{9}$$

By defining $E_0 = E_{for} + 2E_c - E_{d1} - E_{d2}$, Eq. (9) can be expressed as

$$[V^{++}] \propto p(O_2)^{-1/2}\exp(-[E_0 - 2(E_c - E_F)]/kT). \tag{10}$$

Equation (10) shows clearly that, at a fixed O_2 partial pressure and in equilibrium, the oxygen vacancies density increases exponentially as E_F goes down in band gap, which results in the impossibility to have a constant doping level along the whole space charge region. The latter assumption is the basis of the widely acknowledged depletion approximation (DA); Eq. (10) sets important limitations to it in the case of mobile donors. As an alternative approach to derive Eq. (10), we can consider that the density of lattice vacancies is given by[15]

$$[V] \propto \exp(-E_{for}/kT), \tag{11}$$

where, as before, E_{for} is the vacancy formation energy, the energy needed to take an atom from a lattice site inside the crystal to the vapor phase. The reactions that lead to Eq. (11) are the following:

$$O_0 + S \Longleftrightarrow V + O_s^o, \tag{12}$$

in which an oxygen atom is taken from a lattice site inside the crystal and landed at the surface, and Eq. (6), in which an adsorbed oxygen atom desorbs to the gas phase. The corresponding mass action law for the reaction given in Eq. (12) can be written as

$$\frac{[V].[O_s^0]}{[S]} \propto \exp(-E_{sur}/kT), \tag{13}$$

where E_{sur} is the energy needed to take an oxygen atom from a lattice site inside the crystal to the surface. On the other hand, the mass action law for Eq. (6) is

$$\frac{p(O_2)^{1/2}.[S].}{[O_s^0]} \propto \exp(-E_{ads}/kT), \tag{14}$$

where E_{ads} is the oxygen desorption energy.

Combining Eqs. (13) and (14), we can find an explicit relation between $[V]$ and $p(O_2)$

$$[V] \propto p(O_2)^{-1/2}\exp(-(E_{sur} + E_{ads})]/kT). \tag{15}$$

As before, we have a vacancy in the crystal that behaves as a donor that ionizes giving two electrons away. Electrons relaxed to the Fermi level leading to an energy gain $E_{d1} + E_{d2} - 2E_F$. Thus, noting that $E_{for} = E_{sur} + E_{ads}$, $[V^{++}]$

adopts the form of Eq. (9). Finally, by considering that $E_0 = E_{for} + 2E_c - E_{d1} - E_{d2}$, we derive again Eq. (10). With this second derivation of Eq. (10), it is clearer that the formation energy of an ionized donor increases with the position of E_F with respect to the bands. This is why it is usually stated that the density of ionized vacancies decreases exponentially with the Fermi level.[16]

Based on Eq. (10), for a given gas phase pressure, $[V^{++}]$ can be expressed as a function of band bending as

$$[V^{++}] = N_d \exp[2(E_c(x) - E_{cb})/kT], \tag{16}$$

where N_d denotes the vacancy concentration in the bulk, $E_c(x)$ is the bottom of the conduction band, and E_{cb} is the bottom of the conduction band in the bulk as shown in Fig. 1.

INTERGRANULAR BARRIERS

It is surprising that researchers in the field regularly adopt intergranular barriers with parabolic shape assuming a constant doping along the grains.[5] Note that Eq. (16) clearly states that the equilibrium vacancy concentration, and then of dopants, strongly depends on band bending. Interestingly, Romppainen and Lantto have raised the issue long time ago.[6] They originally considered a temperature high enough allowing sufficiently mobility to ionized oxygen vacancies. If so, they will tend to move toward the surface due to the present electric field, which rearrange the vacancies. Eventually, there will be a concentration gradient responsible for a diffusion of vacancies in the opposite direction than that originated by the electric field. This constitutes a third manner to show that vacancies form an ideal solution with a concentration adopting the form

$$[V^{++}] = N_d \exp(2eV(x)/kT). \tag{17}$$

Note that Eqs. (16) and (17) are equivalent because the potential near the surface $V(x)$ can be described as the changes of the bottom of the conduction band $E_C(x) - E_{Cb}$. After having demonstrated the equivalence of the approaches, in what follows, we will follow Lantto's work and his notation[6] to describe the effect of oxygen in- and out-diffusion in the formation of intergranular barrier.

Now, assuming that oxygen vacancies are the only relevant charged particles (strictly, this is only valid for fully depleted slabs[17]) by resorting to the Poisson's equation the potential $V(x)$ can be deduced to be

$$V(x) = \frac{kT}{2e} \ln\left[1 + \tan^2\left(\frac{x}{\sqrt{2}L_D}\right)\right], \tag{18}$$

where $L_D = (ekT/4e^2N_d)^{1/2}$ is the Debye length. In Fig. 2, we plot $V(x)$ as a function of $x' = x/2^{1/2}L_D$. The resulting barrier radically differs from the parabolic shaped barrier of the DA. In the inset, the same barrier profile is shown in log-log scale; the non-parabolic character and the abruptness of the barrier close to the surface become apparent.

The width of the depletion region can be determined resorting to charge neutrality, i.e., the amount of negative charge at the surface must be equal to the amount of positive charge at the depletion region,

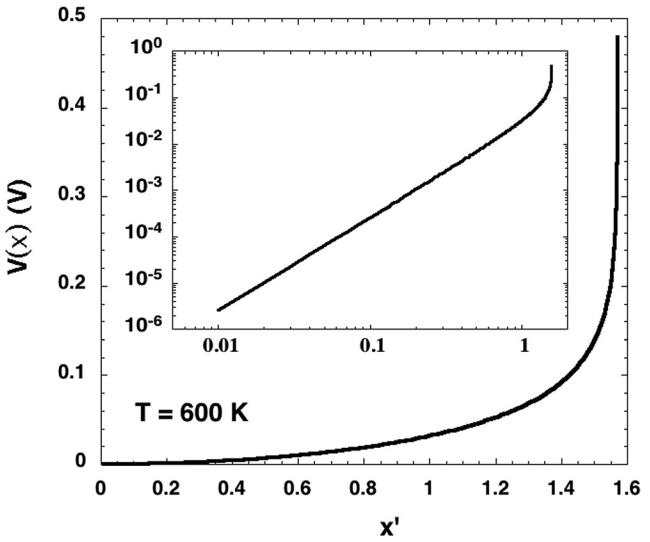

FIG. 2. Profile of the potential near the surface due to band bending. The variable $x' = x/2^{1/2}L_D$, with L_D being the Debye length. The inset shows the same potential in a log-log scale to show the abruptness of the potential.

$$x_0 = \sqrt{2}L_D \arctan\left(\frac{N_t}{2\sqrt{2}N_d L_D}\right), \tag{19}$$

where N_t is the density of trapped electrons at the surface. Now, with Eqs. (18) and (19) the height of the surface potential energy barrier is obtained

$$V_s = \frac{kT}{2e} \ln\left[1 + \frac{N_t}{8N_d^2 L_D^2}\right]. \tag{20}$$

CALCULATION OF SCHOTTKY BARRIERS HEIGHTS

Assuming we are dealing with a non-degenerate n-type semiconductor, the density of electrons at the conduction band is given by

$$n = N_c \exp\left(-\frac{E_c - E_F}{kT}\right), \tag{21}$$

where N_c is the effective density of states in the conduction band.

From Eq. (10), the vacancy concentration in the bulk can be expressed as

$$N_d = Cp(O_2)^{-1/2} \exp(-[E_0 - 2(E_{cb} - E_F)]/kT), \tag{22}$$

where C is a constant.

Assuming all oxygen vacancies are doubly ionized, the neutrality condition allows us to equate Eqs. (21) and (22), $n = 2N_d$. Then, the position of the Fermi level with respect to the conduction band in the bulk can be determined as

$$E_{cb} - E_F = \frac{E_0 - kT \ln(2Cp(O_2)^{-1/2}/N_c)}{3}. \tag{23}$$

It rests to obtain an explicit relation between the oxygen gas pressure and the amount of ionized oxygen at the surface. At temperatures between 100 and 500 °C, oxygen shows ionosorption. At temperatures below 150 °C, the molecular form dominates and above this temperature the monatomic form dominates.[3] Thus, considering that oxygen is adsorbed monatomically, we can write

$$O_2 \Longleftrightarrow 2O_s^0. \tag{24}$$

Assuming a low coverage, the corresponding mass action law for the reaction can be written as

$$\frac{[O_s^0]^2}{p(O_2)} \propto \exp(E_{ads}/kT). \tag{25}$$

The ratio between ionized and neutral oxygen atoms at the surface depends on the Fermi level position as

$$\frac{[O_s^-]}{[O_s^0]} = \exp[-(E_t - E_F)/kT], \tag{26}$$

where E_t is the ionization level.

Finally, with Eqs. (25) and (26), noting that the density of ionized oxygen atoms at the surface was named N_t, we can write

$$N_t = Ap(O_2)^{1/2}\exp[-(eV_s + E_{cb} - E_F - E_{ads}/2)/kT], \tag{27}$$

where A is a constant.

Knowing the parameters involved, with Eqs. (20)–(23) and (27), the surface potential energy barrier and the Schottky barrier can be determined as a function of temperature and oxygen pressure.

Some of the needed parameters have been estimated by Maier and Gopel; from Ref. 18 $E_{ads} = 2$ eV and $E_0 = 2.2$ eV. To work out the equations, we will assume, as an example, that for a given oxygen pressure p_0 at $T = 600$ K, $N_d = 10^3$ 1/m^3, and $N_t = 10^{17}$ 1/m^2. These values were chosen because they lead to regularly observed barrier heights. First, assuming all oxygen vacancies are doubly ionized, with Eq. (21) we can determine the bulk Fermi level position in the gap. Knowing $E_{cb} - E_F$, the constants C in Eq. (22) and A in Eq. (27), with the help of Eq. (20), can be determined.

In Fig. 3, we plot Schottky barrier heights as a function of pressure that results of our modeling considering that the system is in equilibrium (filled line). This means that once all involved parameters are determined, we first find as a function of the relative pressure, the Fermi level position with Eq. (23). Then, the vacancy concentration in the bulk with Eq. (22), the density of ionized oxygen atoms at the surface with Eq. (27), and the height of the surface potential energy barrier with Eq. (20). Finally, the Schottky barrier height results from the sum of $E_{cb} - E_F$ and eV_s.

Recent reported results by Barsan *et al.* show a change in work function of ≈53 meV at 300 °C after a relative change in pressure by a factor of 20.[19] Note that changes in work function can be considered to directly reflect changes in the Schottky barrier height. Similar change in the relative pressure gives in our model a change in Schottky barrier height of 58 meV, a result that seems remarkable given all the assumptions and approximations introduced and the complexities of the experiments.

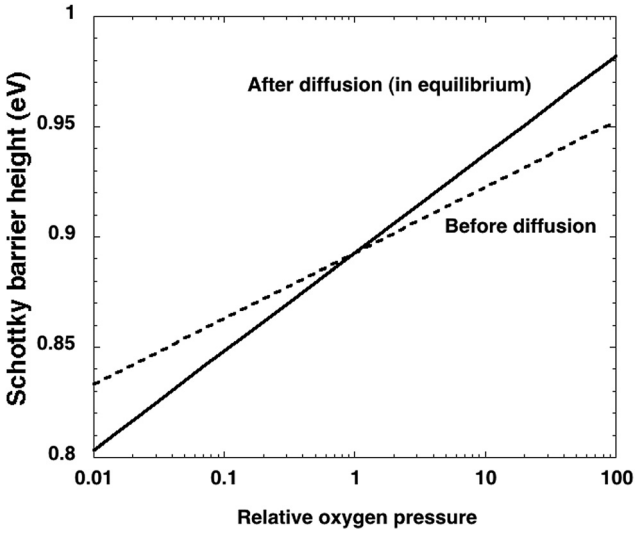

FIG. 3. Schottky barrier height as a function of the relative oxygen pressure. The filled line corresponds to the equilibrium doping of the sensor. The dashed line is the Schottky barrier height keeping the doping constant and equal to that of the reference pressure.

In Fig. 3, we also present the Schottky barrier heights as a function of pressure for a constant doping profile (dashed line). Specifically, calculations were performed keeping the doping that corresponds to the reference pressure p_0. The goal is to describe the response of the sensor after a sudden change in oxygen pressure. Starting from the reference pressure with the sensor in equilibrium with the ambient, suppose that the oxygen pressure is suddenly increased. The regularly observed rapid increase of resistivity indicates that equilibrium at the surface is rapidly reached; the Schottky barrier height would increase as described by the dashed line. Thus, due to a higher barrier height and wider depletion layer, the sample resistivity increases. Interestingly, it has been observed that after this rapid change, there is a subsequent slow evolution of the sensor resistivity. We proposed that, at high enough temperature (>200 °C), oxygen diffusion into the grains is responsible for these slow changes as they affect the oxygen vacancy concentration. Consistently with this interpretation, our model predicts, as oxygen diffuses into the sensor and the doping decreases, a subsequent increase of the Schottky barrier height that reflects in an increase of resistivity. Under some circumstances, it is possible to observe a slow decrease in resistivity. A plausible explanation for this phenomenon has been given recently and it is out of the scope of the present work.[14]

CONCLUSIONS

This work points to the basic understanding of the intergranular barriers responsible for gas sensing. The presented model unifies three different approaches to the same physical phenomenon. The recalled mechanism leads to a modified

approximation with respect to the normally acknowledged one, to deal with intergranular Schottky barriers at the interface of SnO_2 nano-grains in oxygen atmosphere. It leads to results consistent with experimental observations made by other groups. Despite the many complexities involved, the basic relations among the relevant parameters allow one to deduce the consequences of a relative change in the oxygen pressure. Specifically, Schottky barrier changes could be determined as a consequence of a relative change in the ambient oxygen pressure. This is valid for any pressure as long as the assumptions of the model are valid. Indeed, the model has many limitations. It is not valid for very low oxygen pressure because at some point surface states play a role. (Note that for $p(O_2) = 0$, the model predicts no band bending!) It is also not valid for large oxygen pressure because the assumptions adopted for the oxygen adsorption are not valid.

[1]N. Yamazoe, Sens. Actuators B **108**, 2 (2005).
[2]W. Göpel and K. D. Schierbaum, Sens. Actuators B **26–27**, 1 (1995).
[3]N. Barsan and U. Weimar, J. Electroceram. **7**, 143 (2001).
[4]L. M. Cukrov, P. G. McCormick, K. Galatsis, and W. Wlodarski, Sens. Actuators B **77**, 491 (2001).
[5]M. J. Madou and R. Morrison, *Chemical Sensing with Solid State Devices* (Academic, San Diego, 1989), p. 6.
[6]P. Romppainen and V. Lantto, J. Appl. Phys. **63**, 5159 (1988).
[7]T. G. G. Maffeïs, G. T. Owen, C. Malagù, G. Martinelli, M. K. Kennedy, F. E. Kruis, and S. P. Wilks, Surf. Sci. **550**, 21 (2004).
[8]B. Kamp, R. Merkle, and J. Maier, Sens. Actuators B **77**, 534 (2001).
[9]T. Sahm, A. Gurlo, N. Barsan, and U. Weimar, Sens. Actuators B **118**, 78 (2006).
[10]M. S. Castro and C. M. Aldao, Appl. Phys. Lett. **63**, 1077 (1993).
[11]G. Blaustein, M. S. Castro, and C. M. Aldao, Sen. Actuators B **55**, 33 (1999).
[12]M. A. Ponce, C. Malagù, M. C. Carotta, G. Martinelli, and C. M. Aldao, J. Appl. Phys. **104**, 054907 (2008).
[13]C. Malagù, G. Martinelli, M. A. Ponce, and C. M. Aldao, Appl. Phys. Lett. **92**, 162104 (2008).
[14]C. M. Aldao, D. A. Mirabella, M. A. Ponce, A. Giberti, and C. Malagù, J. Appl. Phys. **109**, 063723 (2011).
[15]C. Kittel, *Introduction to Solid State Physics* (John Wiley & Sons, 1976), Chap. 17.
[16]F. Oba, M. Choi, A. Togo, A. Seko, and I. Tanaka, J. Phys.: Condens. Matter **22**, 384211 (2010).
[17]W. Izydorczyk, Phys. Status Solidi B **248**, 694 (2011).
[18]J. Maier and W. Gopel, J. Solid State Chem. **72**, 293 (1988).
[19]N. Barsan, M. Hübner, and U. Weimar, Sens. Actuators B **157**, 510 (2011).